DOI: 10.1002/zaac.200900503

Synthesis, Structural Characterization and Luminescence Studies of Di- and Trinuclear Gold(I) Alkynyl-phosphine Complexes

Igor O. Koshevoy,[a] Laura Koskinen,[a] Ekaterina S. Smirnova,[a,c] Matti Haukka,[a] Tapani A. Pakkanen,[a] Alexei S. Melnikov,[b] and Sergey P. Tunik*[c]

Keywords: Polynuclear complexes; Akynyl ligands; Luminescence; Gold; NMR spectroscopy

Abstract. Reactions of the polymer $\{Au^{I}C_2Ph\}_n$ with polyphosphine ligands [1,4-bis(2-diphenylphosphino-1H-imidazol-1-yl)-benzene (dpib), 1,3,5-tris(4-diphenylphosphinophenyl)benzene (tppb), 2,2'-bis(diphenylphosphanyl)-4,4'-bipyridine (dpbp), and 3,6-bis(diphenylphosphanyl)pyridazine (dppz)] afforded four gold(I) alkynyl-polyphosphine complexes $[\{AuC_2Ph\}_2(\mu\text{-dpib})]$ (**1**), $[\{AuC_2Ph\}_3(\mu_3\text{-tppb})]$ (**2**), $[\{AuC_2Ph\}_2(\mu\text{-dpbp})]$ (**3**), and $[\{AuC_2Ph\}_2(\mu\text{-dppz})]$ (**4**) in nearly quantitative yield. The compounds obtained were characterized using elemental analysis, ESI-MS, X-ray crystallography, and polynuclear NMR spectroscopy. Intermolecular aurophilic interaction together with π–π and σ–π stacking build up the supramolecular 3D network of complex **3**, whereas none of these intermolecular bondings were found in the crystal structures of compounds **1**, **2**, and **4**. Complexes **1**–**4** are luminescent both in solution (CH_2Cl_2) and in solid state under laser irradiation (λ_{ex} = 308 nm). In solution, the diphosphine complexes **1**–**4** display dual emission corresponding to ligand centered transitions (λ_{em} = 360–375 nm) along with weaker contribution from MLCT excited states at ca. 490 nm. The long wavelength component of the emission plays a dominant role in the solid state luminescence spectra of complexes **1**, **3**, and **4** (460, 544, 520 nm, respectively) whereas the triphosphine complex **2** shows dual luminescence (372 and 520 nm) with considerable contribution from ligand centered excited state.

Introduction

Synthesis, molecular structure, and reactivity of gold(I) alkynyl-phosphine complexes attract growing attention because of their unique photophysical properties [1–11] and ability to build up supramolecular polynuclear ensembles based on auro(metallo)philic interaction [5, 6, 12–15]. These polymetallic aggregates are very often stabilized by bridging ligands of various natures, of which polyphosphines are most widely used. Chemical and physical properties of the resulting compounds are determined to a large extent by the nature of bridging ligands, their electronic and, particularly, steric characteristics, which play a decisive role in the design of supramolecular architecture.

In the present communication we report the synthesis of two di- and triphosphine ligands: 1,4-bis(2-diphenylphosphino-1H-imidazol-1-yl)-benzene (dpib) and 1,3,5-tris(4-diphenylphosphinophenyl)benzene (tppb), which contain extended aromatic spacers between the coordinating phosphorus atoms. Four polynuclear gold(I) alkynyl-phosphine complexes based on these ligands and on two other diphosphines reported earlier [16, 17] were prepared and structurally characterized. Their absorption and emission spectra were studied and compared with those of the closely analogous mononuclear gold(I) alkynyl-phosphine compounds.

Results and Discussion

Synthesis of Phosphine Ligands

Two novel phosphine ligands: 1,4-bis(2-diphenylphosphino-1H-imidazol-1-yl)-benzene (dpib) and 1,3,5-tris(4-diphenylphosphinophenyl)benzene (tppb), have been synthesized by re-

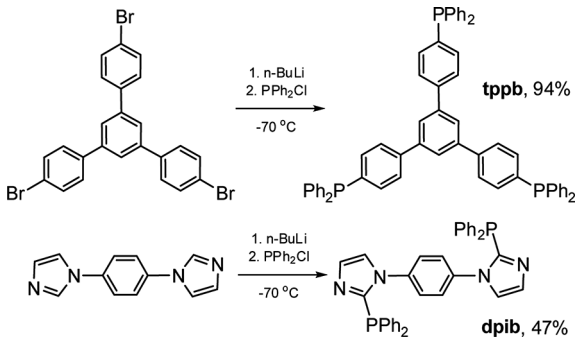

Scheme 1. Synthesis of phosphine ligands (dpib) and (tppb).

* Dr. S. P. Tunik
Fax: +7-812-4286939
E-Mail: stunik@inbox.ru
[a] Department of Chemistry
University of Joensuu
Joensuu, 80101, Finland
[b] Department of Physics
St.-Petersburg State University
Ulijanovskaja 3
198504, St. Petersburg, Russia
[c] Department of Chemistry
St.-Petersburg State University
Universitetskii pr. 26
198504, St.-Petersburg, Russia

action of the corresponding organic precursors with *n*-BuLi followed by addition of the corresponding amount of Ph_2PCl (Scheme 1) in moderate and excellent yield, respectively. Composition and structure of these compounds were established using elemental analysis and ^{1}H-NMR spectroscopy. The data obtained (see Experimental Section) are in complete agreement with the structures shown in Scheme 1.

Synthesis and Structural Characterization of Complexes 1–4

Reactions of phenylacetylene-gold polymer with a stoichiometric amount of di(tri)-phosphines afford di- and trinuclear gold alkynyl-phosphine complexes in nearly quantitative yield (Scheme 2).

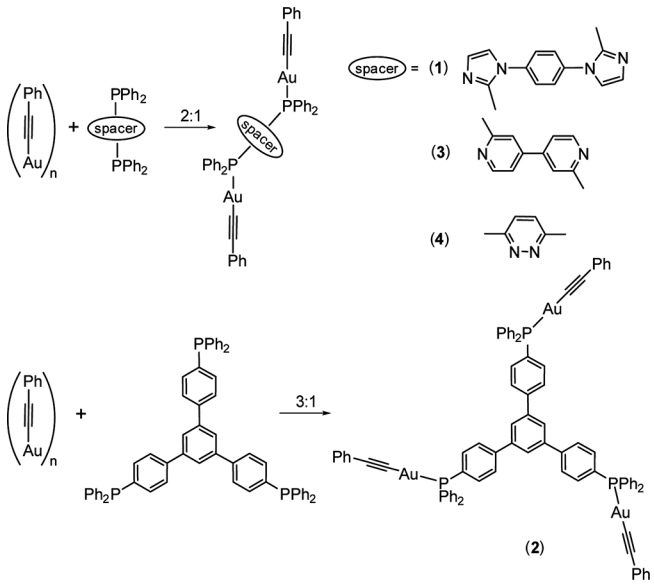

Scheme 2. Synthesis of the gold complexes **1**–**4**.

The solid state structures of the compounds obtained were established using X-ray crystallography, crystal data are summarized in Table 1. ORTEP views of the molecular structures of complexes **1**–**4** are shown in Figure 1, Figure 2, Figure 3, and Figure 4, the main structural parameters are given in captions to the figures.

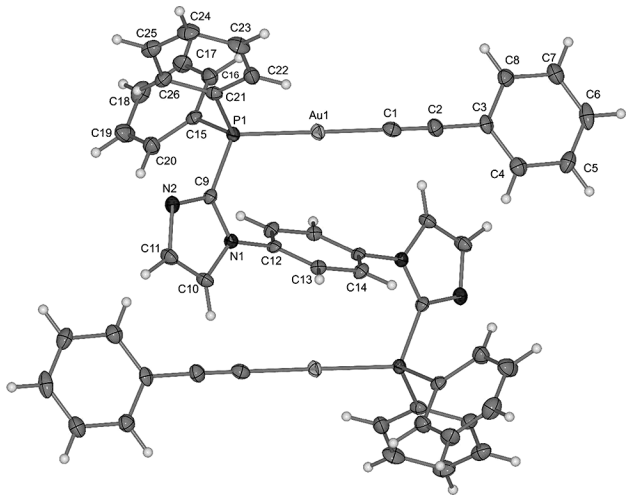

Figure 1. ORTEP view of the structure of **1**. Selected structural parameters: Au(1)–C(1) 2.001(4) Å, Au(1)–P(1) 2.2712(9) Å, C(1)–C(2) 1.202(5) Å, C(2)–C(1)–Au(1) 175.0(3)°, C(1)–Au(1)–P(1) 178.19(10)°.

In the obtained complexes the phosphine ligands bridge two (**1**, **3**, **4**) and three (**2**) Au^I atoms, which are also bound to the alkynyl ligands to give molecules with several chromophoric gold(I) atoms. Coordination of the gold-alkynyl fragment to

Table 1. Crystallographic data for complexes **1**–**4**.

	1	**2**	**3**	**4**
empirical formula	$C_{52}H_{38}Au_2N_4P_2$	$C_{91}H_{68}Au_3P_3$	$C_{62}H_{50}Au_2N_2OP_2$	$C_{44}H_{32}Au_2N_2P_2$
formula weight	1174.74	1845.26	1294.91	1044.59
temp /K	120(2)	120(2)	120(2)	100(2)
λ /Å	0.71073	0.71073	0.71073	0.71073
crystal system	Triclinic	Monoclinic	Monoclinic	Triclinic
space group	$P\bar{1}$	$P2_1/c$	$C2/c$	$P\bar{1}$
a /Å	8.3182(4)	25.5244(5)	22.1340(11)	10.4098(7)
b /Å	10.6887(3)	17.5430(4)	11.4410(7)	12.0023(5)
c /Å	12.1967(5)	15.9046(3)	20.7580(8)	15.8675(14)
α /°	88.373(2)	90	90	84.864(5)
β /°	87.413(2)	91.4014(10)	99.707(3)	77.967(5)
γ /°	85.265(2)	90	90	68.410(4)
V /Å^3	1079.28(7)	7119.5(3)	5181.4(5)	1802.7(2)
Z	1	4	4	2
ρ_{calc} /Mg m^{-3}	1.807	1.722	1.660	1.924
μ(Mo-K_α) /mm^{-1}	6.905	6.282	5.762	8.252
No. reflns.	19103	78662	30312	34411
Unique reflns.	4928	12477	5927	8976
GOOF (F^2)	1.071	1.014	1.102	1.060
R_{int}	0.0404	0.0721	0.0518	0.0329
R_1[a)] ($I \geq 2\sigma$)	0.0266	0.0626	0.0350	0.0226
wR_2[b)] ($I \geq 2\sigma$)	0.0521	0.1575	0.0724	0.0381

a) $R_1 = \Sigma\|F_o|-|F_c\|/\Sigma|F_o|$.b) $wR_2 = [\Sigma[w(F_o^2-F_c^2)^2]/\Sigma[w(F_o^2)^2]]^{1/2}$.

Zeitschrift für anorganische und allgemeine Chemie ZAAC Journal of Inorganic and General Chemistry

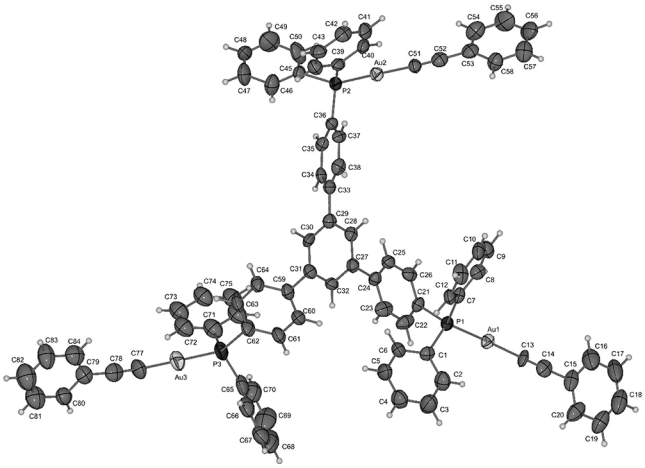

Figure 2. ORTEP view of the structure of **2**. Selected structural parameters: Au(1)–C(13) 1.981(11) Å, Au(2)–C(51) 2.006(12) Å, Au(3)–C(77) 1.988(15) Å, Au(1)–P(1) 2.269(3) Å, Au(2)–P(2) 2.277(3) Å, Au(3)–P(3) 2.266(4) Å, C(1)–Au(1)–P(1) C13–Au1–P1 177.5(4)°, C51–Au2–P2 175.5(3)°, C77–Au3–P3–179.6(5)°, C(14)–C(13)–Au(1) 178.9(12)°, C(52)–C(51)–Au(2) 169.2(11)°, C(78)–C(77)–Au(3) 173.9(14)°.

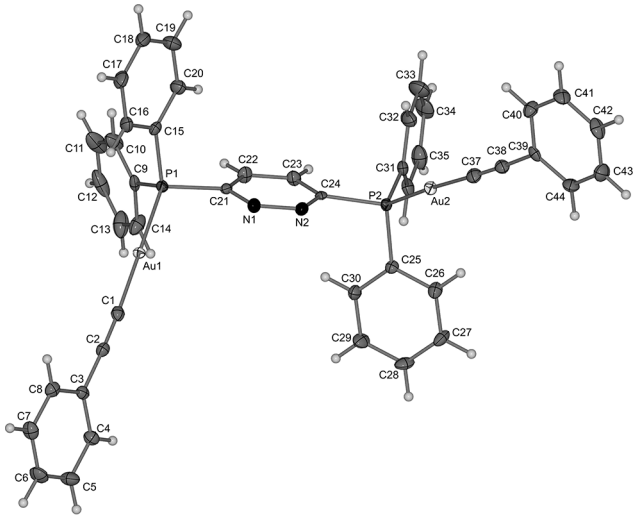

Figure 4. ORTEP view of the structure of **4**. Selected structural parameters: Au(1)–C(1) 1.991(3) Å, Au(1)–P(1) 2.2613(9) Å, C(1)–C(2) 1.196(5) Å, C(1)–Au(1)–P(1) 175.6°, C(2)–C(1)–Au(1) 177.0(3)°.

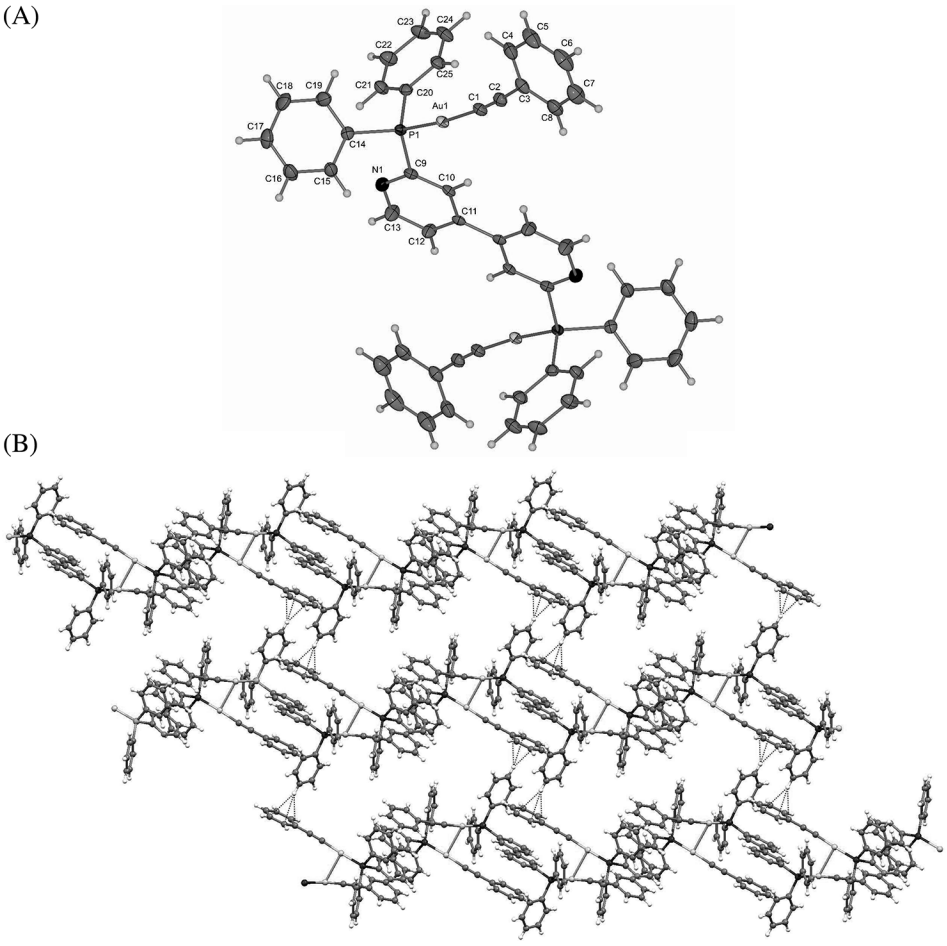

Figure 3. (A) ORTEP view of the structure of **3**. (B) 3D network formed by the molecules of **3** in the solid state. Selected structural parameters: Au(1)–C(1) 1.995(5) Å, Au(1)–P(1) 2.2663(12) Å, C(1)–C(2) 1.203(7) Å, Au–Au 2.990(7) Å, C(2)–C(1)–Au(1) 174.2(4)°, C(1)–Au(1)–P(1) 174.69(14)°.

the phosphorus functions of the bridging polyphosphine ligands to form di- and trinuclear complexes is the general structural motif of the studied molecules. The arrangement around the Au^I atoms is expectedly very close to linear and gold to ligand bond lengths, Au–C(alkynyl) (1.981–2.006 Å), Au–P (2.2613–2.2770) Å, fall in the range typical for the other gold(I) alkynyl-phosphine complexes, see for example [14, 18, 19]. Unusual *zig-zag* conformation of the molecule in complex **1** is very probably dictated by minimization of intramolecular hindrance between essentially nonlinear 1,2-substituted phenylene-bis(imidazole) spacer and phenyl substituents at the phosphorus atoms.

In compound **2**, the aromatic rings of the 1,3,5-tris(4-phenyl)benzene spacer are not coplanar in the crystal cell and evidently are able to rotate freely around single C–C bonds in solution that points to the lack of conjugation in this system and apparently makes all three gold(I) atoms independent chromophores. The molecular conformation of compound **4** shown in Figure 4 is very similar to the structures found earlier [19, 20] for other diphosphines with linear 1,4-phenylene spacers. Free rotation around single P–C bond between the phosphorus atom and the phenylene spacer of the diphosphine is allowed. It is evident that because of structural constraints none of the complexes under study is able to form intramolecular aurophilic bonds, which were found earlier for molecules of this sort [21, 14, 22] on the basis on the polyphosphine backbones, which can bring the gold atoms into positions favorable for Au^I–Au^I bond formation. The structures of compounds **1**, **2**, and **4** do not display intermolecular aurophilic interactions [13, 23] and make possible formation of either molecular dimers [20, 24–27] or solid state supramolecular structures [18]. In contrast to the structures of compounds **1**, **2**, and **4**, the crystal packing of complex **3** results in formation of an infinite "staircase-like" chain of the molecules bound to each other through Au^I–Au^I bonds (2.99 Å) and face-to-face interaction between 1,4-bpy spacers and phenyl rings of the alkynyl ligands as shown in Figure 3, (B). These aromatic systems are nearly coplanar with distances of 4.2–4.5 Å between the corresponding planes. This observation clearly points to π-stacking interaction, which strengthens bonding in the molecular chain. Moreover, these chains are additionally linked to each other through edge-to-face CH-π interactions to form a 3D network. This structural motif looks very similar to the supramolecular design of the crystal structure of Me_3P–Au–$C_2\{C_6H_2Me_2\}C_2$–Au–PMe_3, in which individual molecules are joined together to form an infinite *zig-zag* chain through aurophilic interaction with an intermolecular Au–Au distance of 3.1361(9) Å [18].

The NMR spectroscopic data (see Experimental Section and Figures S1–S3) show that in solution the complexes under study are presented in their molecular form (including **3**) and the structures found in the solid state remain unchanged in solution. The ^{31}P NMR spectra of compounds **1**–**4** display a singlet resonance in the area typical for the phosphines coordinated to gold(I)-alkynyl fragments [5, 20] with a characteristic lowfield coordination shift relative to the starting phosphines. Careful assignment of the proton spectra was performed on the basis of ^1H COSY experiments (Figures S1–S3) and comparison of the data obtained with the previously reported spectroscopic characteristics of closely analogous diphosphine-gold complexes [5, 20]. In the ^1H NMR spectra of compounds **1**–**4** a set of high field resonances (7.50–7.25 ppm), which represent an "*ortho-meta-para*" combination according to the ^1H COSY spectra, evidently belongs to the phenyl rings of the alkynyl ligands. In turn a more complicated set of the lowfield signals (8.90–7.2 ppm) displays 2D connectivity and ^{31}P–^1H coupling constants corresponding to the protons of phenyl rings and spacers of the phosphine ligands. Relative intensities and multiplicities of the signals fit well the molecular structures found in the solid state.

The UV/Vis spectra of complexes **1**–**4** in CH_2Cl_2 (Table 2) display quite similar spectroscopic patterns in the near UV region (230–300 nm). All spectra show strong absorption bands in the range 265–285 nm together with higher energy (HE) UV absorption at shorter wavelength. The former bands are usually assigned to the transition from σ(Au–P) orbital to an empty π* antibonding orbital centered at aryl fragments of either phosphine or alkynes, whereas HE absorption is associated with π–π* intraligand transitions in this type of complexes [2, 14, 19, 28]. The tails of lower energy bands extend down to 370 nm and may mask very weak absorption originated from metal centered electronic transitions.

Excitation of complexes **1**–**4** with λ_{ex} = 308 nm both in solid state and in solution showed relatively weak blue-green luminescence (see Figure 5 and Table 2). In dichloromethane solution (Figure 5 B) all complexes show dual emission with the more intense short wavelength component at 375.5, 360, 375.5, 377 nm for **1**–**4**, respectively. The less intensive long wavelength component is substantially redshifted to appear at ca. 490 nm. A similar type of dual luminescence behavior was

Table 2. Spectroscopic data of **1**–**4** in degassed CH_2Cl_2 and in solid state at 298 K.

Complex		λ_{abs} /nm ($10^{-5}\varepsilon$ /$cm^{-1}\cdot m^{-1}$)	λ_{em} /nm (λ_{ex} = 308 nm)
1	solution	256sh (0.65), 268.5 (0.68), 282 (0.52)	375.5, 491
	solid state		421, 442, 451, 462, 487
2	solution	270.5 (1.1), 282.5 (1.1)	360, 490
	solid state		371.5, 520
3	solution	239 (5.2), 270 (3.4), 282 (3.3)	375.5, 491
	solid state		544
4	solution	282sh (1.9), 238 (2.7), 269 (2.2)	377, 491
	solid state		520

Zeitschrift für anorganische und allgemeine Chemie ZAAC Journal of Inorganic and General Chemistry

already found for analogous gold(I) alkynyl-polyphosphine complexes: (PhC_2Au-)(dppe) [24], $PhC_2Au–Ph_2P–C_6H_4PPh_2–Au–C_2Ph$ [19], and {PhC_2Au-}$_4$[1,4,8,11-tetra(diphenylphosphinomethyl)-1,4,8,11-tetraazacyclotetradecane] [27] in dichloromethane solution. In these cases the higher energy emission was assigned to $\pi \rightarrow \pi^*$ intraligand excited states in the aromatic rings of phenylalkynyl and phosphine ligands.

In the case of linear diphosphine complex $PhC_2Au–Ph_2P–C_6H_4PPh_2–Au–C_2Ph$ [19], the low energy emission band was assigned to $\sigma(Au–P) \rightarrow \pi^*(Ar_{bridge})$ transitions localized onto aryl moieties of the bridging phosphine ligand. However, in the case of (PhC_2Au-)(dppe) [24], and the tetranuclear gold-tetraphosphine complex {PhC_2Au-}$_4$[1,4,8,11-tetra(diphenylphosphinomethyl)-1,4,8,11-tetraazacyclotetradecane] [27],

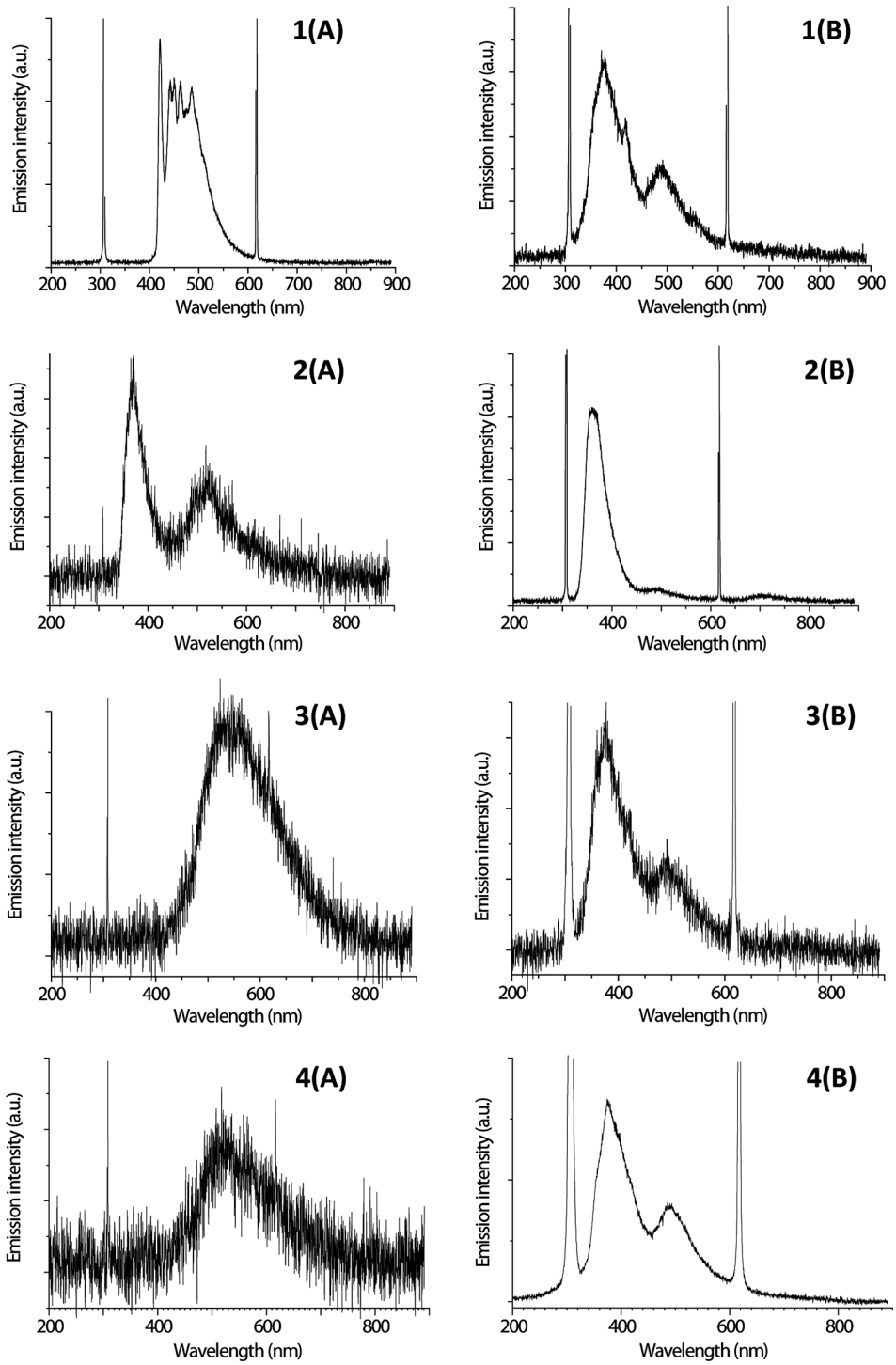

Figure 5. Emission spectra of complexes **1**–**4** in solid state (A) and in CH_2Cl_2 solution (B) at 25 °C, λ_{ex} = 308 nm.

which show intramolecular aurophilic contacts, the long wavelength emission can be assigned to the triplet state $(d_{\delta^*})^1(p_\sigma)^1$ localized onto the orbitals responsible for intramolecular Au–Au bonds [24] or for the formation of oligomeric aurophilic aggregates [27]. This suggestion is strongly supported by the concentration dependence of relative intensities of the low (560 nm) and high (425 nm) energy emission bands in the dichloromethane solution of the latter compound [27], which display substantial growth of the low energy emission component with an increase in the complex concentration. This experimental observation is in agreement with the system description, which includes formation of supramolecular aggregates supported by aurophilic interactions between the molecules under study and a shift of the reaction equilibrium to the aggregation at higher complex concentrations. Moreover, for the alkynyl-polyphosphine complexes containing intramolecular aurophilic bonds, one can observe the only low energy emission in the 500–750 nm range [28]. For complexes **1**–**4**, the formation of aurophilic supramolecular aggregates in solution looks hardly probable for **1**, **2**, and **4** and the weak low energy emission bands should be assigned to $\sigma(Au–P)\rightarrow\pi^*(Ar_{bridge})$ excited states. In the case of complex **3**, the solid-state structure of this complex points to the possibility to form supramolecular aurophilic bonding additionally supported by π–π and π–σ stacking. Thus, the origin of the long wave length emission for **3** (which is very similar to that observed in the solid state samples) can be assigned either to $\sigma(Au–P)\rightarrow\pi^*(Ar_{bridge})$ excited states or to the transitions localized inside aurophilic $\{Au_2\}$ fragments, similar to the assignment made in the earlier works [24, 27].

Solid state emission spectra of compounds **1**–**4** are shown in Figure 5 A. Complex **1** displays strong emission in the range 400–600 nm, which can be interpreted as a combination of a vibronic-structured band between 400 and 500 nm and long wavelength shoulder with the maximum at ca. 500 nm. Vibrational progression spacing of ca. 1000 nm may be interpreted as metal perturbed vibrational spectrum of excited state aromatic moieties in **1** that is completely in line with the assignment of this emission to $\pi \rightarrow \pi^*$ intraligand excited states analogously to the interpretation of solution luminescence given above. Similarly, the low energy shoulder in this emission spectrum can be assigned to $\sigma(Au–P) \rightarrow \pi^*(Ar_{bridge})$ excited states. The trinuclear complex **2** displays unstructured dual emission with short and long wavelength components centered at 371 and ca. 520 nm, respectively, in solid state. Their assignment is evidently analogous to that one for emission bands observed for complex **1**. In contrast to compounds **1** and **2**, the solid state luminescence spectra of complexes **3** and **4** display only long wavelength bands at ca. 544 and ca. 520 nm, respectively. In the case of complex **3**, major contribution of the low energy emission is probably related to the formation of a supramolecular structure, which is shown in Figure 3, where emission from $\pi \rightarrow \pi^*$ intraligand excited states is effectively quenched because of π-stacking and edge-to-face CH-π interactions in the crystal cell. In turn, the low energy emission ascribed to the transitions localized at the $\{Au_2\}$ fragment (see above) is relatively enhanced because of complete involvement of the central gold atoms into aurophilic interaction.

Experimental Section

General Comments

Au(tht)Cl (tht = tetrahydrothiophene) [29], $(AuC_2Ph)_n$ [30], 2,2'-bis(diphenylphosphanyl)-4,4'-bipyridine (dpbp) [16], 3,6-bis(diphenylphosphanyl)pyridazine (dppz) [17], 1-[4-(1H-imidazol-1-yl)phenyl]-1H-imidazole [31], and 1,3,5-tris(4-bromophenyl)benzene [32] were synthesized according to published procedures. Preparation of the phosphines was carried out in a nitrogen atmosphere. Tetrahydrofurane was distilled over Na-benzophenoneketyl in a nitrogen atmosphere prior to use. Other reagents and solvents were used as received. Solution ^1H, ^{13}C, and ^{31}P NMR spectra were recorded with Bruker Avance 400 and Bruker DPX 300 spectrometers. The chemical shifts /ppm were referenced to residual solvent resonances and external 85 % H_3PO_4 in the ^1H, ^{13}C, and ^{31}P spectra, respectively. The 2D COSY spectra were run using standard Bruker pulse sequence. Microanalyses were carried out in the analytical laboratory of St.-Petersburg State University. UV/Vis spectra were recorded with a Shimadzu UV 3600 spectrophotometer.

Synthesis

1,4-Bis(2-diphenylphosphino-1H-imidazol-1-yl)-benzene (dpib): 1-[4-(1H-imidazol-1-yl)phenyl]-1H-imidazole (1 g, 4.76 mmol) was suspended in THF (100 cm^3), the mixture was cooled to –78 °C and a 1.6 M solution of *n*-BuLi in hexane (8 cm^3, 12.8 mmol) was added within 5 min. The orange mixture was stirred below –70 °C for 1.5 h. Afterwards, neat PPh_2Cl (2.6 g, 11.8 mmol) was added dropwise. The reaction mixture was stirred at this temperature for further 1 h and was afterwards slowly warmed to room temperature and left overnight whilst stirring. The reaction was quenched by addition of solid NH_4Cl. Afterwards, the volatiles were evaporated, the orange-brown residue was washed with methanol (3 × 20 cm^3), diethyl ether (10 cm^3) and dried. The crude product was extracted with CH_2Cl_2 (3 × 10 cm^3), diluted with diethyl ether (3 cm^3) and the solution was passed through a layer of silica gel (70–230 mesh, 2 × 5 cm). The solvents were evaporated, the colorless solid was washed with methanol once again and vacuum dried. Yield 1.3 g (47 %). Analytically pure sample was obtained by recrystallization from CH_2Cl_2/hexane. Anal. $C_{36}H_{28}N_4P_2$: calcd. C 74.73; H 4.88; N 9.68 %; found: C 74.65; H 4.92; N 9.70 %. **$^{31}P\{^1H\}$ NMR** ($CDCl_3$): δ = –29.5 (s). **^1H NMR** ($CDCl_3$): δ = 7.25 (s, -C_6H_4-, 4 H), 7.29 (dd, (-P-$C_3N_2H_2$), 2 H, *J*(H-H) 1.2, *J*(P-H) 1.9 Hz), 7.33–7.38 (m, Ph, 12 H), 7.41 (d, (-P-$C_3N_2H_2$), 2 H, *J*(H-H) 1.2 Hz), 7.42–7.49 (m, Ph, 8 H).

1,3,5-Tris(4-diphenylphosphinophenyl)benzene (tppb): 1,3,5-tris(4-bromophenyl)benzene (1.55 g, 2.86 mmol) was dissolved in THF (40 cm^3), the solution was cooled down to –78 °C and a 1.6 M solution of *n*-BuLi in hexane (7 cm^3, 11.2 mmol) was added within 5 min. A pale suspension was formed and stirred below –70 °C for 2 h. Afterwards, neat PPh_2Cl (2.5 g, 11.3 mmol) was added dropwise. The resulting yellow solution was stirred at this temperature for further 1 h and slowly warmed to room temperature. The solution was left overnight whilst stirring. Afterwards, the pale-yellow solution was filtered and the solvents were removed under vacuo. The solid residue was washed with methanol (3 × 20 cm^3), diethyl ether-hexane mixture (1:2 v/v, 2 × 15 cm^3) and vacuum dried. A colorless solid was obtained and dissolved in CH_2Cl_2 (ca. 50 cm^3), passed through a layer

Zeitschrift für anorganische und allgemeine Chemie ZAAC Journal of Inorganic and General Chemistry

of Silica (70–230 mesh, 2 × 5 cm), diluted with hexane (20 cm^3) and evaporated to give microcrystalline product of sufficient purity. Yield 2.3 g (94 %). Analytically pure sample was obtained by a chromatographic separation on Silica [3 × 20 cm, eluent CH_2Cl_2-hexane (3:4, v/v)] and subsequent recrystallization from THF/methanol. Anal. $C_{60}H_{45}P_3$: calcd. C 83.91; H 5.24 %; found: C 83.03; H 5.43 %. **$^{31}P\{^1H\}$ NMR** ($CDCl_3$): δ = –6.1 (s). **^1H NMR** ($CDCl_3$): δ = 7.80 (s, -C_6H_3-, 3 H), 7.67 (dd, *meta*-H, (-C_6H_4-P), 6 H, *J*(H-H) 8.2, *J*(P-H) 1.4 Hz), 7.43 (m, *ortho*-H, (-C_6H_4-P), 6 H, *J*(H-H), *J*(P-H) 8.0 Hz), 7.40–7.37 (m, Ph, 30 H).

[{AuC_2Ph}$_2$(μ-dpib)] (1): (AuC_2Ph)$_n$ (110 mg, 0.369 mmol) was suspended in CH_2Cl_2 (20 cm^3) and dpib (112 mg, 0.192 mmol) was added to the reaction mixture. The yellow suspension turned into a colorless transparent solution within a few minutes. The reaction mixture was diluted with toluene (10 cm^3) and stirred for 30 min in the absence of light. The resulting solution was passed through Al_2O_3 (0.5 × 2 cm, neutral, ≈ 150 mesh) and concentrated to ca. 5 cm^3. A colorless microcrystalline solid was precipitated by centrifugation, washed with toluene (5 cm^3), diethyl ether (2 × 5 cm^3) and vacuum dried. Yield 212 mg (94 %). Single crystals of **1** suitable for X-ray analysis were grown by slow evaporation of CH_2Cl_2/toluene solution at room temperature. Anal. $C_{50}H_{38}N_4Au_2P_2$: calcd. C 52.17; H 3.30; N 4.87 %; found: C 52.07; H 3.45; N 4.71 %. **$^{31}P\{^1H\}$ NMR** ($CDCl_3$): δ = 12.0 (s, br). **^1H NMR** ($CDCl_3$): diphosphine: δ = 7.34 (s, -C_6H_4-, 4 H), 7.76 (d, (-P-$C_3N_2H_2$), 2 H, *J*(H-H) 1,5 Hz), 7.20 (d, (-P-$C_3N_2H_2$), 2 H, *J*(H-H) 1.5 Hz), 7.72 (m, *ortho*-H, (Ph-P), 8 H, *J*(H-H) 8.5, *J*(P-H) 12 Hz), 7.47 (t, *para*-H, (Ph-P), 4 H, *J*(H-H) 7.6 Hz), 7.51 (m, *meta*-H, (Ph-P), 8 H, *J*(H-H) 8.6, 7.6, *J*(P-H) 2 Hz); {$Au(C_2Ph)$}$_2$: δ = 7.37 (m, orto/*meta*-H, 4 H), 7.26 (m, orto/*meta*-H, 4H + *para*-H, 6 H).

[{AuC_2Ph}$_3$(μ$_3$-tppb)] (2): (AuC_2Ph)$_n$ (110 mg, 0.369 mmol) was suspended in CH_2Cl_2 (10 cm^3). tppb (113 mg, 0.132 mmol) was added to the suspension to give a colorless transparent solution within a few minutes. The reaction mixture was diluted with toluene (10 cm^3) and stirred for 30 min. in the absence of light. The resulting solution was passed through Al_2O_3 (0.5 × 2 cm, neutral, ≈ 150 mesh) and concentrated to ca. 5 cm^3. A colorless microcrystalline solid was precipitated by centrifugation, washed with toluene (5 cm^3), diethyl ether (2 × 5 cm^3) and vacuum dried. Yield 196 mg (93 %). Single crystals of **2** suitable for X-ray analysis were grown by slow evaporation of CH_2Cl_2/toluene solution at room temperature. Anal. $C_{84}H_{60}P_3Au_3$: calcd. C 57.55; H 3.45 %; found: C, 58.01; H, 3.67 %. **$^{31}P\{^1H\}$ NMR** ($CDCl_3$): δ = 41.8 (s). **^1H NMR** ($CDCl_3$): diphosphine: δ = 7.81 (s, -C_6H_3-, 3 H), 7.77 (dd, *meta*-H, (-C_6H_4-P), 6 H, *J*(H-H) 8.3, *J*(P-H) 2 Hz), 7.69 (m, *ortho*-H, (-C_6H_4-P), 6 H, *J*(H-H) 8.3, *J*(P-H) 12 Hz), 7.67 (m, *ortho*-H, (Ph-P), 12 H, *J*(H-H) 8.5, *J*(P-H) 12.2 Hz), 7.54 (t, *para*-H, (Ph-P), 6 H, *J*(H-H) 6.8 Hz), 7.51 (m, *meta*-H, (Ph-P), 12 H, *J*(H-H) 8.5, 6.8, *J*(P-H) 2 Hz); {$Au(C_2Ph)$}$_3$: δ = 7.47 (m, orto/*meta*-H, 6 H), 7.25 (m, orto/*meta*-H, 6H + *para*-H, 3 H).

[{AuC_2Ph}$_2$-(μ-dpbp)] (3): (AuC_2Ph)$_n$ (110 mg, 0.369 mmol) was suspended in CH_2Cl_2 (10 cm^3). dpbp (101 mg, 0.192 mmol) was added and yellow suspension turned into a colorless transparent solution within minutes. It was diluted with toluene (10 cm^3) and stirred for 30 min. in the absence of light. The resulting solution was passed through Al_2O_3 (0.5 × 2 cm, neutral, ≈ 150 mesh) and concentrated to ca. 5 cm^3. A pale-yellow microcrystalline solid was precipitated by centrifugation, washed with toluene (5 cm^3), diethyl ether (2 × 5 cm^3) and vacuum dried. Yield 198 mg (92 %). Analytically pure sample was obtained by recrystallization from CH_2Cl_2/toluene. Single crystals of **3** suitable for X-ray analysis were grown by slow evaporation of CH_2Cl_2/benzene solution in 5 °C. Anal. $C_{50}H_{36}N_2Au_2P_2$: calcd. C 53.57; H 3.21; N 2.50 %; found: C 53.62; H 3.34; N 2.25 %. **$^{31}P\{^1H\}$ NMR** ($CDCl_3$): δ = 42.2 (s). **^1H NMR** ($CDCl_3$): diphosphine: δ = 8.90 (d, 2 H, (P-(NC_5H_3), 2 H, *J*(H-H) 5.0 Hz), 8.16 (m, 2 H, (P-(NC_5H_3)), *J*(H-P) 7.7, ^4J (H-H) 1 Hz), 7.52 (m, 2 H, (P-(NC_5H_3)), 7.8 (m, *ortho*-H, (Ph-P), 8 H, *J*(H-H) 8.6, *J*(P-H) 12 Hz), 7.26 (t, *para*-H, (Ph-P), 4 H, *J*(H-H) 7.6 Hz), 7.51 (m, *meta*-H, (Ph-P), 8 H, *J*(H-H) 8.6, 7.6, *J*(P-H) 2 Hz); {$Au(C_2Ph)$}$_2$: δ = 7.50 (m, *meta*-H + *ortho*-H, 8 H), 7.26 (m, *para*-H, 2 H).

[{AuC_2Ph}$_2$(μ-dppz)] (4): (AuC_2Ph)$_n$ (110 mg, 0.369 mmol) was suspended in CH_2Cl_2 (10 cm^3). dppz (86 mg, 0.192 mmol) was added to the suspension to give a colorless transparent solution within a few minutes. It was diluted with toluene (10 cm^3) and stirred for 30 min. in the absence of light. The resulting solution was passed through Al_2O_3 (0.5 × 2 cm, neutral, ≈ 150 mesh) and concentrated to ca 5 cm^3. A colorless microcrystalline solid was precipitated by centrifugation, washed with toluene (5 cm^3), diethyl ether (2 × 5 cm^3) and vacuum dried. Yield: 182 mg (91 %). Analytically pure sample was obtained by recrystallization from CH_2Cl_2/hexane at room temperature. Single crystals of **4** suitable for X-ray analysis were grown by slow evaporation of CH_2Cl_2/hexane solution at room temperature. Anal. $C_{44}H_{32}N_2Au_2P_2$: calcd. C 50.57; H 3.06; N 2.68 %; found: C 50.57; H 3.41; N 2.61 %. **$^{31}P\{^1H\}$ NMR** ($CDCl_3$): δ = 40.2 (s). **^1H NMR** ($CDCl_3$): diphosphine: δ = 7.95 (m, -$C_4H_2N_2$-, 2 H, *J*(H-H) 8.0, ^3J(P-H) 4.7, ^4J(P-H) 4.6 Hz), 7.80 (m, *ortho*-H, (Ph-P), 8 H, *J*(H-H) 8.4, *J*(P-H) 13, *J*(P-H) 2 Hz), 7.56 (t, *para*-H, (Ph-P), 4 H, *J*(H-H) 7.6 Hz), 7.51 (m, *meta*-H, (Ph-P), 8 H, *J*(H-H) 8.4, 7.6, *J*(P-H) 2 Hz); {$Au(C_2Ph)$}$_2$: δ = 7.49 (m, orto/*meta*-H, 4 H), 7.24 (m, orto/*meta*-H, 4H + *para*-H, 2 H).

Photophysical Measurements

An Excimer laser LPX 100 (Lambda Physik) was used to induce luminescence. Laser pulse duration was 35 ns, pulse energy 160 mJ, repetition rate 1–25 Hz, excitation wavelength 308 nm. Emission spectra were recorded with a SD2000 spectrometer (Ocean Optics). Halogen lamp LS-1-CAL (Ocean Optics) and deuterium lamp DH2000 (Ocean Optics) were used to calibrate the absolute spectral response of the spectral system in the range 200–875 nm. All solutions were carefully degassed before measurements.

X-ray Structure Determinations

The crystals of compounds **1**–**4** were immersed in cryo-oil, mounted in a Nylon loop, and measured at a temperature of 100–120 K. The X-ray diffraction data were collected with a Nonius KappaCCD diffractometer using Mo-K_α radiation (λ = 0.710 73 Å). The *Denzo-Scalepack* [33] or *EvalCC* [34] program packages were used for cell refinements and data reductions. The structures were solved by direct methods using the *SHELXS-97* [35] program with the *WinGX* [36] graphical user interface. A semi-empirical absorption correction (*SADABS*) [37] was applied to all data. Structural refinements were carried out using *SHELXL-97* [35]. The low data quality and high residual electron density in complex **4** was due to the weakly diffracting crystal. Also, in complex **4** the carbon atoms in toluene of crystallization were refined with equal anisotropic displacement parameters. In complex **2** the H_2O hydrogen atoms were located from the difference Fourier map but constrained to ride on their parent atom, with U_{iso} = 1.5. Other hydrogen atoms were positioned geometrically and constrained to ride on their parent atoms, with C–H = 0.95–0.98 Å and U_{iso} = 1.2–1.5 U_{eq} (parent atom). The crystallographic details are summarized in Table 1. Selected bond lengths and angles are given in figure captions.

CCDC-751649, CCDC-751650, CCDC-751651, and CCDC-751652 (**1**–**4**) contain the supplementary crystallographic data for this paper. These data can be obtained free of charge from The Cambridge Crystallographic Data Centre, 12 Union Road, Cambridge CB21EZ via www.ccdc.cam.ac.uk/data_request/cif (Fax: +44-1223-336-033; E-Mail: deposit@ccdc.cam.ac.uk).

Acknowledgement

Financial support from *Academy of Finland* (I.O.K.), *Russian Foundation for Basic Research* (grants 09-03-91279 INISa, 09-03-12309) and *Russian Science and Innovation Federal Agency* (contract 02.513.12.3088) is gratefully acknowledged.

References

[1] V. W.-W. Yam, K. K.-W. Lo, *Mol. Supramol. Photochem.* **1999**, *4*, 31–112.
[2] V. W.-W. Yam, K. K.-W. Lo, K. M.-C. Wong, *J. Organomet. Chem.* **1999**, *578*, 3–30.
[3] V. W.-W. Yam, C.-L. Chang, L. C.-K. Chang, K. M.-C. Wong, *Coord. Chem. Rev.* **2001**, *216–217*, 173–206.
[4] V. W.-W. Yam, K.-L. Cheung, E. C.-C. Cheng, N. Zhu, K.-K. Cheung, *Dalton Trans.* **2003**, 1830–1835.
[5] I. O. Koshevoy, A. J. Karttunen, S. P. Tunik, M. Haukka, S. I. Selivanov, A. S. Melnikov, P. Y. Serdobintsev, M. A. Khodorkovskiy, T. A. Pakkanen, *Inorg. Chem.* **2008**, *47*, 9478–9488.
[6] I. O. Koshevoy, A. J. Karttunen, S. P. Tunik, M. Haukka, S. I. Selivanov, A. S. Melnikov, P. Y. Serdobintsev, T. A. Pakkanen, *Organometallics* **2009**, *28*, 1369–1376.
[7] X. He, E. C.-C. Cheng, N. Znu, V. W.-W. Yam, *Chem. Commun.* **2009**, 4016–4018.
[8] V. W.-W. Yam, E. C.-C. Cheng, *Top. Curr. Chem.* **2007**, *281*, 269–309.
[9] V. W.-W. Yam, E. C.-C. Cheng, *Chem. Soc. Rev.* **2008**, *37*, 1806–1813.
[10] N. J. Long, C. K. Williams, *Angew. Chem. Int. Ed.* **2003**, *42*, 2586–2617.
[11] C. E. Powell, M. G. Humphrey, *Coord. Chem. Rev.* **2004**, *248*, 725–756.
[12] M. Bardaji, A. Laguna, *Eur. J. Inorg. Chem.* **2003**, 3069–3079.
[13] P. Pyykko, *Angew. Chem. Int. Ed.* **2004**, *43*, 4412–4456.
[14] V. W.-W. Yam, K.-L. Cheung, S.-K. Yip, K.-K. Cheung, *J. Organomet. Chem.* **2003**, *681*, 196–205.
[15] S.-Y. Yu, Q.-F. Sun, T. K.-M. Lee, E. C.-C. Cheng, Y.-Z. Li, V. W.-W. Yam, *Angew. Chem. Int. Ed.* **2008**, *47*, 4449–4607.
[16] I. O. Koshevoy, M. Haukka, T. A. Pakkanen, S. P. Tunik, P. Vainiotalo, *Organometallics* **2005**, *24*, 3516–3526.
[17] Z.-Z. Zhang, H.-K. Wang, Y.-J. Shen, H.-G. Wang, R.-J. Wang, *J. Organomet. Chem.* **1990**, *381*, 45–52.
[18] M. J. Irwin, J. J. Vittal, R. J. Puddephatt, *Organometallics* **1997**, *16*, 3541–3547.
[19] V. W.-W. Yam, S. W.-K. Choi, K.-K. Cheung, *Organometallics* **1996**, *15*, 1734–1739.
[20] I. O. Koshevoy, L. Koskinen, M. Haukka, S. P. Tunik, P. Y. Serdobintsev, A. S. Melnikov, T. A. Pakkanen, *Angew. Chem. Int. Ed.* **2008**, *47*, 3942–3945.
[21] X. Hong, K.-K. Cheung, C.-X. Guo, C.-M. Che, *J. Chem. Soc., Dalton Trans.* **1994**, 1867–1871.
[22] C.-K. Li, X.-X. Lu, K. M.-C. Wong, C.-L. Chan, N. Zhu, V. W.-W. Yam, *Inorg. Chem.* **2004**, *43*, 7421–7430.
[23] H. Schmidbaur, A. Schier, *Chem. Soc. Rev.* **2008**, *37*, 1931–1951.
[24] D. Li, X. Hong, C.-M. Che, W.-C. Lo, S.-M. Peng, *J. Chem. Soc., Dalton Trans.* **1993**, 2929–2932.
[25] V. W.-W. Yam, W.-K. Lee, *J. Chem. Soc., Dalton Trans.* **1993**, 2097–2100.
[26] V. W.-W. Yam, T.-F. Lai, C.-M. Che, *J. Chem. Soc., Dalton Trans.* **1990**, 3747–3752.
[27] B.-C. Tzeng, W.-C. Lo, C.-M. Che, S.-M. Peng, *Chem. Commun.* **1996**, 181–182.
[28] V. W.-W. Yam, W.-K. Lee, K.-K. Cheung, B. Crystall, D. Phillips, *J. Chem. Soc., Dalton Trans.* **1996**, 3283–3287.
[29] R. Uson, A. Laguna, M. Laguna, *Inorg. Synth.* **1989**, *26*, 85–91.
[30] G. E. Coates, C. Parkin, *J. Chem. Soc.* **1962**, 3220–3226.
[31] H.-J. Cristau, P. P. Cellier, J.-F. Spindler, M. Taillefer, *Chem. Eur. J.* **2004**, *10*, 5607–5622.
[32] J. Brunel, O. Mongin, A. Jutand, I. Ledoux, J. Zyss, M. Blanchard-Desce, *Chem. Mater.* **2003**, *15*, ,.
[33] Z. Otwinowski,W. Minor, *Processing of X-ray Diffraction Data Collected in Oscillation Mode* in: *Methods in Enzymology, Volume 276, Macromolecular Crystallography, Part A*, (Eds.: C. W. Carter, J. Sweet), Academic Press, New York, USA **1997**, pp. 307–326.
[34] A. J. M. Duisenberg, L. M. J. Kroon-Batenburg, A. M. M. Schreurs, *J. Appl. Crystallogr.* **2003**, *36*, 220–229.
[35] G. M. Sheldrick, *Acta Crystallogr., Sect. A* **2008**, *64*, 112–122.
[36] L. J. Farrugia, *J. Appl. Crystallogr.* **1999**, *32*, 837–838.
[37] G. M. Sheldrick, *SADABS-2008/1*, Bruker AXS Area Detector Scaling and Absorption Correction, Bruker AXS: Madison, Wisconsin, USA, **2008**.

Received: October 25, 2009
Published Online: January 7, 2010

